Journal of Electrical Engineering, Electronics, Control and Computer Science – JEEECCS, Volume 9, Issue 31, pages 29-36, 2023

Simulation of the Rotor Side Vector Control of a DFIG Under Different Wind Speeds

Anshu Prakash Murdan[1*], Iqbal Jahmeerbacus[1], S Z Sayed Hassen[1]
[1]Department of Electrical and Electronic Engineering, University of Mauritius
Reduit, Mauritius
Corresponding author email: a.murdan@uom.ac.mu

Abstract **– This paper focuses on the investigation of the performance of rotor side vector control of Doubly-Fed Induction Generators (DFIGs) used in wind turbines. These are widely utilised due to their low cost, high efficiency, and reliability. However, the dynamic behavior of DFIGs under varying wind speeds and grid conditions poses significant challenges in terms of stability. To address these issues, rotor side vector control is commonly employed. In this study, we present a review of existing research on rotor side vector control of DFIGs and provide an overview of the basic principles of DFIG operation and vector control concepts. The study analyzes the impact of various control parameters on the system performance under different wind speeds. The results suggest that rotor side vector control can improve the performance of DFIGs, and optimal control parameters depend on specific operating conditions. This study provides insights for the design, control, and optimization of DFIG-based wind energy conversion systems.**

Keywords-component; Doubly-fed induction generator; Rotor side vector control; Wind power system; Operating conditions

I. INTRODUCTION

Wind energy is rapidly becoming one of the primary sources of renewable energy worldwide, and Doubly-Fed Induction Generators (DFIGs) are widely used in wind turbines due to their low cost, high efficiency, and reliability [1]. DFIGs are capable of operating under variable wind speeds and provide reactive power support to the grid [2]. However, the dynamic behaviour of DFIGs under varying wind speeds and grid conditions poses significant challenges in terms of stability and efficiency. One of the key methods to improve the performance of DFIGs is rotor side vector control [3], which involves controlling the rotor currents and voltages in order to minimize the impact of grid disturbances. Rotor side vector control is a complex and nonlinear process that requires accurate modelling, control, and optimization techniques.

In this paper, we investigate the performance of rotor side vector control of a DFIG under different operating conditions, and analyze the impact of different control parameters on the system performance. We first provide an overview of the basic principles of DFIG operation, the basic concepts of vector control, and the challenges and benefits associated with rotor-side vector control. We then present a literature review of existing research on rotor side vector control of DFIGs. Next, we describe the research methodology, which includes developing mathematical models and simulations using MATLAB/Simulink. Finally, we present the results of the study and discuss their implications for the design, control, and optimization of DFIG-based wind energy conversion systems.

The work contributes to a deeper understanding of the challenges and benefits associated with rotor-side vector control, which can help to guide future research and development efforts in this area. The study has broad implications for the design, control, and optimization of DFIG-based wind energy conversion systems, providing insights that could lead to more efficient, stable, and reliable wind power systems.

II. BACKGROUND

A. Doubly-Fed Induction Generators (DFIGs)

Unlike other types of generators, such as synchronous generators, DFIGs are designed to operate at variable speeds, making them ideal for use in wind turbines where wind speeds can vary widely [4]. DFIGs are called "doubly-fed" because they have two sets of windings on the stator, and one set of windings on the rotor. The stator windings are connected directly to the grid, while the rotor windings are connected to the grid through a set of slip rings, brushes. This allows the generator to control the flow of power between the rotor and the grid, which can help to maintain stability in the overall power system.

One of the challenges of using DFIGs is controlling the rotor side voltage and current. To address this challenge, researchers have developed a technique called rotor side vector control, which allows for precise control of the rotor side voltage and current. This technique involves controlling the magnitude and phase angle of the rotor side voltage and current using feedback control loops. By using rotor side vector control, the generator can maintain stable operation even in the face of changes in wind speed and other factors [5].

The classic theory of rotating fields in a DFIG is based on the principle of electromagnetic induction, where a time-varying magnetic field induces an electromotive force (EMF) in the stator and rotor windings. In a DFIG, the magnetic field is generated by the interaction of stator and rotor currents, creating a rotating magnetic field that rotates at the synchronous speed. The rotor speed can be different from the synchronous speed due to the slip, which is a measure of the difference between the rotor's actual speed and the synchronous speed. By controlling the slip and the rotor current through the back-to-back converter, the DFIG can operate efficiently over a wide range of speeds.The speed of the generator is controlled by adjusting the rotor current through the power converter.

B. Review of previous studies on rotor side vector control of DFIGs

Rotor side vector control, also known as field-oriented control (FOC) or decoupled control aims to independently control the active and reactive power generated by the DFIG by decoupling the stator and rotor currents into direct-axis (d-axis) and quadrature-axis (q-axis) components. This enables efficient operation and improved performance of the generator, particularly in variable-speed applications such as wind turbines.

In previous studies on rotor side vector control of DFIGs, researchers have investigated various aspects of the control strategy, including:

1) Control algorithms: Several control algorithms have been proposed and analyzed for implementing rotor side vector control. These algorithms include proportional-integral (PI) controllers [6], proportional-resonant (PR) controllers [7] , and sliding mode controllers [8], among others. Researchers have compared their performance, stability, and robustness to disturbances and parameter uncertainties.
2) Sensorless control: Some studies have focused on the development of sensorless control techniques for DFIGs. These methods estimate the rotor position and speed without using mechanical sensors, reducing costs and increasing reliability. Techniques such as Model Reference Adaptive System (MRAS) [9] and Extended Kalman Filter (EKF) [10] have been proposed and investigated for this purpose.
3) Grid integration and fault ride-through: Researchers have also examined the performance of rotor side vector control in the context of grid integration and fault ride-through capabilities [11]. They have investigated methods to improve the DFIG's ability to withstand voltage dips, frequency fluctuations, and other grid disturbances while maintaining stability and power quality [12].
4) Optimization: Some studies have focused on optimizing the rotor side vector control strategy for various objectives, such as maximizing power capture, minimizing torque and power oscillations, and enhancing system efficiency [13]. For instance, in [14], the authors proposed an adaptive backstepping control structure, to cater for nonlinearities, as well as uncertainties in the wind power system. To deal with similar issues, other researchers have proposed predictive algorithms based on tip-speed ratio maximum power point tracking (MPPT) [15].

Many previous studies have also compared the performance of DFIGs with rotor side vector control to other types of generators, such as permanent magnet synchronous generators (PMSGs) and synchronous generators (SGs). These comparisons have shown that DFIGs with rotor side vector control can provide comparable or better performance under varying wind speeds and load conditions, making them a viable option for wind power systems [16] [17]. In [18], the authors propose a new method for managing rotor-tied doubly fed induction generators using field-oriented control and a high gain observer. This approach enables wind turbines to operate at variable speeds, thereby enhancing wind energy extraction efficiency. The method's superiority over other observer-based control techniques was confirmed through simulations and comparisons. Furthermore, a novel technique based on the command-filtered integral backstepping principle for controlling the rotor side converter of a wind energy conversion system was developed in [19]. Unlike the traditional backstepping controller, this approach eliminates errors caused by input signal differentiation and stabilizes rotor speed through electromagnetic torque control. Similarly, researchers in [20] aimed to improve the low-voltage ride-through (LVRT) capability of a doubly fed induction generator (DFIG) for maintaining grid stability during transient conditions. Their approach involves modifying the control structure of the DFIG converter to effectively manage rotor overcurrents and DC-link voltage fluctuations. To achieve this, additional voltage terms are introduced into the rotor-voltage references, which enhances the transient behavior of the DFIG control system while maintaining the stability of the current loops. Additionally, the proposed methodology significantly reduces electromagnetic torque oscillations during faults. The effectiveness of the improved converter control design in enhancing the LVRT capability of a DFIG was verified through simulations using MATLAB/Simulink.

The control strategy has seen significant development over the years, and it continues to be a subject of active research as researchers seek to improve the performance, efficiency, and reliability of DFIGs in various applications.

III. METHODOLOGY

The DFIG block diagram in Figure 1 features a Rotor Side Control (RSC) and a Grid Side Control (GSC), along with a back-to-back power electronic converter. While the stator windings of the DFIG connect directly to the power grid, the rotor windings link to the grid through a power electronic converter that typically has a capacity of around 30% of the wind turbine's capacity [21]. The electrical power generated from the rotor can be different from the grid frequency. This allows the rotor speed to be adjustable , and different from the synchronous speed. This feature makes the DFIG well suited for operation under varing wind speeds. The grid-side converter ultimately converts the voltages and currents produced by the rotor to the grid frequency. Additionally, the converter can partially regulate the generator's output power, improving power quality and offering some grid support. This approach is cost-effective, as the converter's capacity is relatively small. This is accomplished by implementing slip control, which compensates for any deviations between the rotor's actual speed and the synchronous speed. As a result, the converter can guarantee optimal energy production at the desired frequency and voltage levels, regardless of the rotor's speed.

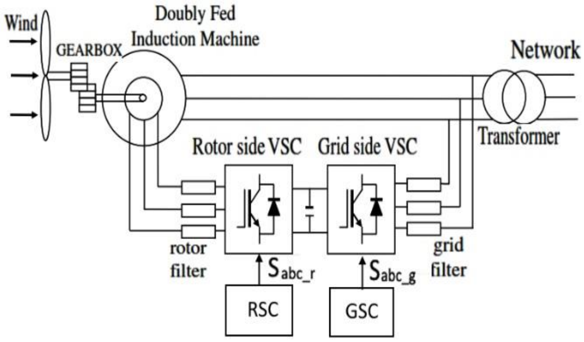

Figure 1.

Figure 1. Variable speed wind turbine with partial-scale power converter and a doubly fed induction generator [22]

A. Reversible Power Electronic Converter

The DFIG is equipped with a reversible power electronic converter that allows for two different modes of operation: rotor side control and grid side control [23].

In rotor side control mode, the power electronic converter is connected to the rotor winding of the DFIG. This allows the converter to control the amount of power flowing through the rotor, thereby regulating the speed and torque of the turbine. By controlling the amount of power flowing through the rotor winding, the converter can vary the rotor's speed, independent of the grid frequency [21]. This feature is particularly useful for wind turbines, as it allows the turbine to operate efficiently over a wide range of wind speeds. In rotor side control mode, the converter can also regulate the reactive power flow from the generator to the grid, helping to stabilize the grid voltage.

On the other hand, in the grid side control mode, the power electronic converter is connected to the grid. The converter controls the active and reactive power flow between the grid and the stator winding of the generator [24]. This mode of operation allows the generator to operate at a constant speed, synchronized with the grid frequency. The converter controls the power flow between the stator and the grid, regulating the active power, and maintaining the required reactive power level. Grid side control mode is particularly useful for grid-connected applications as it allows the generator to deliver power to the grid at the required frequency and voltage levels [25].

B. Grid Side Converter

A simplified model of the grid side converter, filter, and grid is depicted in Figure 2. The filter typically consists of L, LC or even LCL elements. The grid voltage is normally supplied through a transformer, and is assumed to be balanced and sinusoidal.

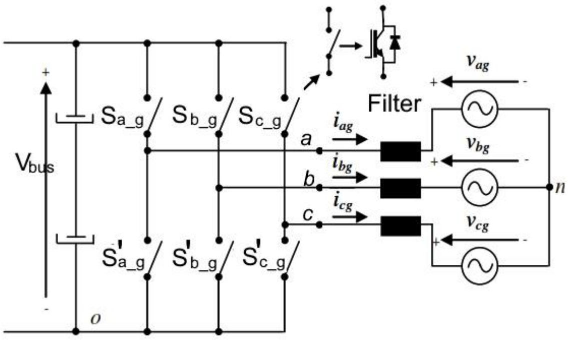

Figure 2 Simplified converter, filter, and grid model

C. Converter Model

The two-level power converter is typically modeled as a set of switches that enable current to flow in either direction. These switches are controlled by signals S_{a_g}, S_{b_g}, and S_{c_g} to regulate the flow of power. Essentially, these signals dictate which switches should be turned on and off at any given time to control the direction and magnitude of current flowing through the converter. In ideal conditions, the following holds:

$$S'_{a\_g} = \overline{S_{a\_g}} \tag{1}$$

$$S'_{b\_g} = \overline{S_{b\_g}} \tag{2}$$

$$S'_{c\_g} = \overline{S_{c\_g}} \tag{3}$$

The converter can produce various output voltages, such as those that are referenced to the DC bus's negative terminal:

$$v_{j0} = V_{bus} S_{j\_g} \quad \text{with } S_{j\_g} \in \{0,1\} \text{ and } j = a,b,c \tag{4}$$

The combination of S_{a_g}, S_{b_g}, and S_{c_g}, can generate AC output voltages with various fundamental frequencies and amplitudes. The converter's output voltages with respect to the grid's neutral point *(n)* are expressed as:

$$v_{jn} = v_{j0} - v_{n0} \quad \text{with } j = a,b,c \tag{5}$$

Assuming a balanced three-phase grid system, we have

$$v_{an} + v_{bn} + v_{cn} = 0 \tag{6}$$

Substituting expression (5) in (6)

$$v_{n0} = \frac{1}{3}(v_{a0} + v_{bo} + v_{co}) \quad (7)$$

Substituting again expression (5) in (7)

$$v_{an} = \frac{2}{3}v_{a0} - \frac{1}{3}(v_{bo} + v_{co}) \quad (8)$$

$$v_{bn} = \frac{2}{3}v_{b0} - \frac{1}{3}(v_{ao} + v_{co}) \quad (9)$$

$$v_{cn} = \frac{2}{3}v_{c0} - \frac{1}{3}(v_{bo} + v_{ao}) \quad (10)$$

Or more simply, directly from the order commands,

$$v_{an} = \frac{V_{bus}}{3}(2S_{a\_g} - S_{b\_g} - S_{c\_g}) \quad (11)$$

$$v_{bn} = \frac{V_{bus}}{3}(2S_{b\_g} - S_{a\_g} - S_{c\_g}) \quad (12)$$

$$v_{cn} = \frac{V_{bus}}{3}(2S_{c\_g} - S_{a\_g} - S_{b\_g}) \quad (13)$$

Table 1 shows eight possible switching states of S_{a_g}, S_{b_g}, and S_{c_g}, leading to eight different output voltage combinations.

TABLE 1 DIFFERENT OUTPUT VOLTAGE COMBINATIONS OF 2L-VSC

S_{a_g} S_{b_g} S_{c_g}	v_{a0}	v_{b0}	v_{c0}	v_{an}	v_{bn}	v_{cn}
0 0 0	0	0	0	0	0	0
0 0 1	0	0	Vbus	-Vbus/3	-Vbus/3	2Vbus/3
0 1 0	0	Vbus	0	-Vbus/3	2Vbus/3	-Vbus/3
0 1 1	0	Vbus	Vbus	-2Vbus/3	Vbus/3	Vbus/3
1 0 0	Vbus	0	0	2Vbus/3	-Vbus/3	-Vbus/3
1 0 1	Vbus	0	Vbus	Vbus/3	-2Vbus/3	Vbus/3
1 1 0	Vbus	Vbus	0	Vbus/3	Vbus/3	-2Vbus/3
1 1 1	Vbus	Vbus	Vbus	0	0	0

D. Rotor Side Converter

Figure 3 depicts the rotor side converter which is similar to the grid side converter. A *dv/dt* filter used to supply the rotor of the DFIG. A two-level voltage source converter is used to feed the rotor, while the *dv/dt* filter is used to protect the machine from the harmful effects caused by the voltage source converter. The filter is typically made up of RC or RLC elements and is designed to prevent issues such as capacitive leakage currents, bearing currents, and increased stress on motor insulation. The DC link, which is the DC part of the back-to-back converter, helps maintain a constant voltage level in its terminals by storing energy in one or more capacitors. The DC link acts as an interface between the rotor and grid side converters.

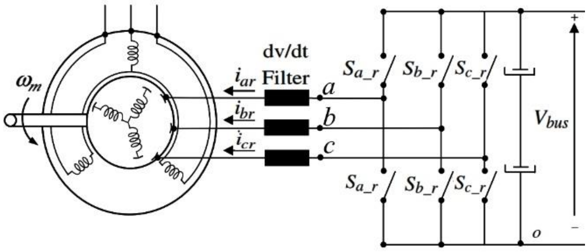

Figure 3 Rotor side converter and dv/dt filter supplying the rotor at the machine[22]

E. Rotor Side Vector Control

The DFIG is vector controlled using a *dq* frame that rotates synchronously, where the *d*-axis aligns with the stator flux space vector. Figure 4 provides a visual representation of this configuration.

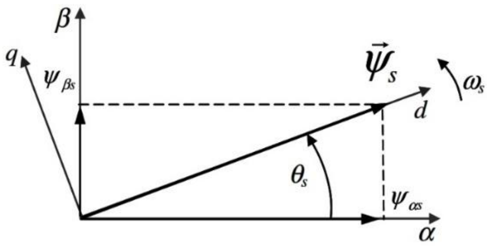

Figure 4 Synchronous rotating *dq* reference frame aligned with the stator flux space vector

The *d-q* model utilizes equivalent circuits to represent the stator and rotor windings, comprising resistances, inductances, and voltages. This model is used to calculate the voltage and current in the stator and rotor windings, along with the machine's generated torque. Optimizing the performance of the DFIG involves adjusting the rotor current using the power converter [26], which affects the machine's torque and speed. The direct rotor current is proportional to the stator reactive power, while the quadrature rotor current is proportional to the active stator power or torque [27]. Consequently, modeling the DFIG in a synchronous reference frame enables the calculation of the rotor voltage, based on the rotor currents and stator flux:

$$v_{dr} = R_r i_{dr} + \sigma L_r \frac{d}{dt} i_{dr} - \omega_r \sigma L_r i_{qr} + \frac{L_m}{L_s}\frac{d}{dt}|\overrightarrow{\psi_s}| \quad (14)$$

$$v_{qr} = R_r i_{qr} + \sigma L_r \frac{d}{dt} i_{qr} + \omega_r \sigma L_r i_{dr} + \omega_r \frac{L_m}{L_s}|\overrightarrow{\psi_s}| \quad (15)$$

If the voltage drop across the stator resistance is negligible, the stator flux is maintained at a constant level [28]. This happens because the stator is connected directly to the grid, which provides a stable and constant AC voltage. As a result, the machine is able to maintain a consistent level of performance, without fluctuations in the stator flux. This means that the term $\frac{d}{dt}\left|\overrightarrow{\psi_s}\right|$ is equal to zero. To regulate dq rotor currents, a controller is used for each current component, based on Equations (14) and (15), as depicted in Figure 6. The control block diagram consists of current loops that operate with rotor currents, referred to the stator side.

IV. MATLAB SIMULATION OF THE ROTOR SIDE VECTOR CONTROL

Matlab/Simulink is used for simulating the rotor-side converter of the DFIG. The simulation assumes that the DC bus voltage of the AC/DC/AC converter is set by the grid-side converter. The DFIG is modeled as an asynchronous machine, and the stator is connected to a programmable three-phase voltage source. The rotor is connected to a power electronic converter that is controlled by a two-level Pulse Width Modulation (PWM) generator. The RSC control block uses field-oriented control for current loops to regulate the RSC. To simplify the simulation, a DC voltage source is used instead of a GSC. The Simulink model is depicted in Figure 5. The simulation has a constant sample time, and the RSC control system is tested under specific conditions to evaluate its performance. Overall, the simulation provides valuable insights into the behavior of the RSC control system and its impact on the performance of the DFIG.

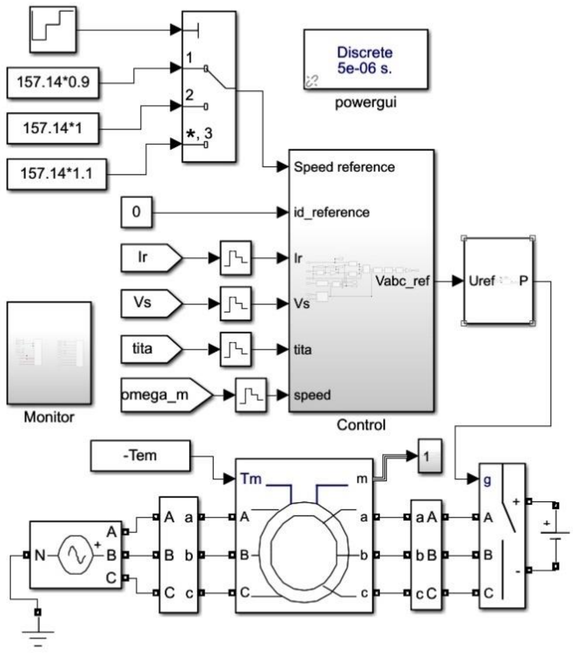

Figure 5 Simulink model of a 2MW DFIG with Rotor side control

A. *Implementation of RSC Control*

To control the DFIG, a vector control system is used in a synchronous reference frame. This system is implemented through a control block, as shown in Figure 7, which sets the initial reference values for the current and speed to zero. In order to determine the necessary control values, the three-phase measurements block provides information about the information is then used to regulate the performance of the DFIG, ensuring that it operates efficiently and effectively.

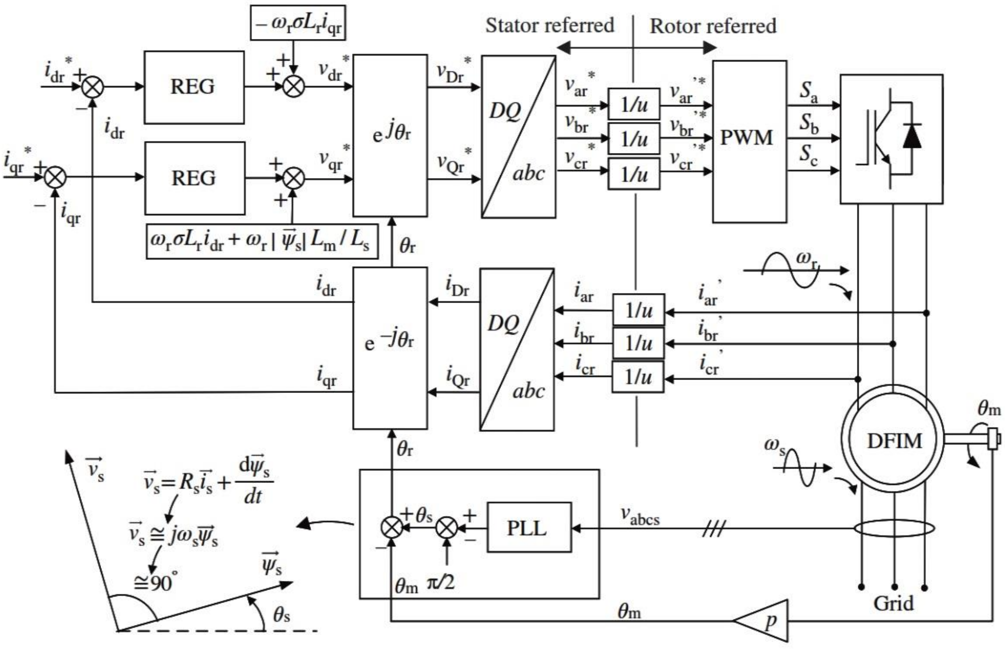

Figure 6 Current control loops of the DFIM [22]

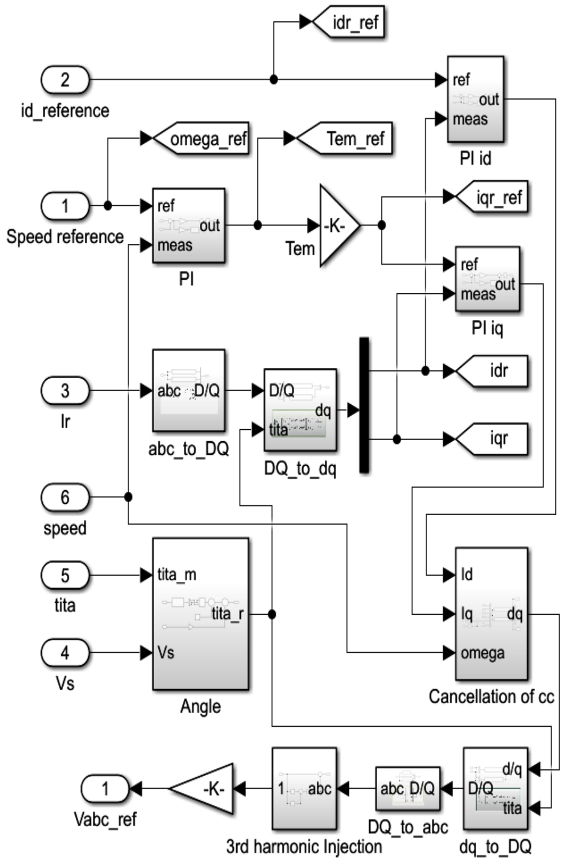

Figure 7 Stator flux-oriented Vector Control of RSC of DFIG

The system uses two control loops to regulate the current and speed of an electric machine. These control loops use various transformation blocks to convert between different reference frames. A PWM generator is used to generate a triangular wave, which is normalized to control the machine's output voltage. The system employs a third harmonic injection technique to enhance the output voltage by 15%. To achieve this, a transformation angle is computed from the stator and rotor angles and used as input to the transformation blocks. The control system utilizes a PI regulator in the outer loop to control the speed of the machine, while two PI regulators are employed in the inner loop to regulate the i_d and i_q currents. The values for the k_p and k_i parameters of the PI regulators are determined based on the transfer function of the system. To ensure optimal performance of the machine, the stator flux-oriented vector control system is utilized.

B. Simulation Results

As shown in Figure 6, the reference speed is varied according to Table 2.

TABLE 2 REFERENCE SPEED VARIATION

Time/s	Reference Speed in terms of synchronous speed
0-2	0.9
2-4	1.0
4-6	1.1

The variations of the actual rotor speed, rotor currents, torque, stator voltage and currents are observed. As depicted in Figure 8(A), the actual speed catches up with the reference speed after a small overshoot. Figure 8(B) shows two signals (i_{qr_ref} and i_{qr}). After a short period of transients at the start of the simulation, the current i_{qr} follows the i_{qr_ref} with very little variations. Figure 8(C) depicts the v_{dr_ref}, which is almost constant at zero V. On the other hand, the torque represented in Figure 8(D), depends on the i_{qr}. At every step change in speed, the torque shows a corresponding overshoot for around 0.25 seconds before stabilizing to its initial value. Figure 8(E) depicts i_{dr_ref} and i_{dr}. The i_{dr_ref} has been maintained at zero, therefore the voltage reference shown in Figure 8(C) has been more or less zero. Also, i_{dr} closely follows i_{dr_ref} due to the action of the PI controller. Figure 8(F) shows the V_{qr_ref} variation. At synchronous speed the average value of V_{qr_ref} is zero. At subsynchronous speed, the latter is positive, while it is negative at supersynchronous speed. The Figure 8(G) shows the stator voltage, which is equal to the grid voltage. The stator and rotor currents are depicted in Figure 8(H) and Figure 8(I) respectively. The simulation shows the effect of drastic change in speed at 2, 4 and 6 seconds. This creates transients in the stator currents, which eventually die out after 0.25 seconds. The frequency of the sinusoidal stator currents is around 50 Hz, irrespective of the rotor speed. The measured values fluctuates between 49.991 and 50.002 Hz. The rotor currents, on the other hand, experience a change in sequence. At subsynchronous speed, the rotor currents are in the *abc* sequence. At synchronous speed, rotor speeds are constant values (dc). The DFIG is working as a synchronous motor, with dc currents at the rotor. And at supersynchronous speed, the currents are again sinusoidal, but in the *acb* sequence. Another set of simulation was carried out by varying the load conditions of the generator, as well as the reference speed. It was observed that the overall variation of the different parameters, as shown in Figure 8 was similar.

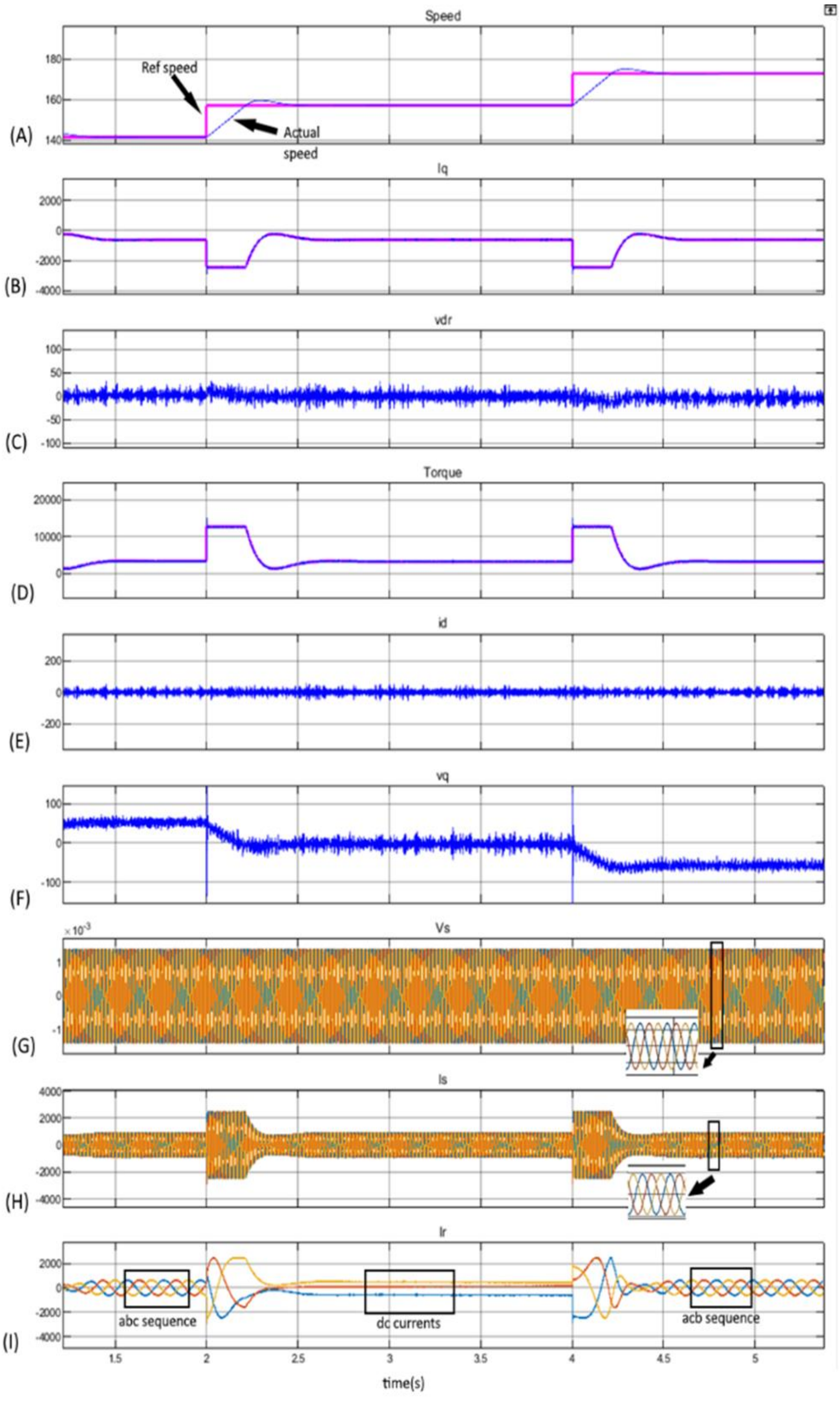

Figure 8 Simulation results for rotor side vector control : (A) Speed, (B) i_(qr_ref) and i_qr, (C) v_(dr_ref), (D) Torque, (E) i_(dr_ref) and i_dr, (F) V_(qr_ref), (G) V_s, (H) I_s, (I) I_r

V. CONCLUSION

In this paper, the modeling and control of a DFIG was performed. Simulation of the rotor side vector control was carried out, using Matlab/Simulink, under different operating conditions of wind speeds and load. The results confirm the proper response of the PI controllers, that enable controlled variables to come closer to their reference values in a very short time. This work also offers valuable insights into the DFIG's performance and its rotor side vector control system in different operating conditions. The study can aid in improving the efficiency, stability, and reliability of wind power systems, which could eventually lead to the development of more cost-effective and sustainable renewable energy sources.

REFERENCES

[1] R. Hemmati, H. Faraji, and N. Y. Beigvand, "Multi objective control scheme on DFIG wind turbine integrated with energy storage system and FACTS devices: Steady-state and transient operation improvement," International Journal of Electrical Power & Energy Systems, vol. 135, p. 107519, 2022, doi: https://doi.org/10.1016/j.ijepes.2021.107519.

[2] S. Gupta and A. Shukla, "Improved dynamic modelling of DFIG driven wind turbine with algorithm for optimal sharing of reactive power between converters," Sustainable Energy Technologies and Assessments, vol. 51, p. 101961, 2022, doi: https://doi.org/10.1016/j.seta.2022.101961.

[3] M. A. S. Ali, K. K. Mehmood, S. Baloch, and C.-H. Kim, "Modified rotor-side converter control design for improving the LVRT capability of a DFIG-based WECS," Electric Power Systems Research, vol. 186, p. 106403, 2020, doi: https://doi.org/10.1016/j.epsr.2020.106403.

[4] B. Desalegn, D. Gebeyehu, and B. Tamirat, "Wind energy conversion technologies and engineering approaches to enhancing wind power generation: A review," Heliyon, vol. 8, no. 11, p. e11263, 2022, doi: https://doi.org/10.1016/j.heliyon.2022.e11263.

[5] H. Benbouhenni and N. Bizon, "Advanced Direct Vector Control Method for Optimizing the Operation of a Double-Powered Induction Generator-Based Dual-Rotor Wind Turbine System," Mathematics, vol. 9, no. 19. 2021. doi: 10.3390/math9192403.

[6] B. Desalegn, D. Gebeyehu, and B. Tamrat, "Evaluating the performances of PI controller (2DOF) under linear and nonlinear operations of DFIG-based WECS: A simulation study," Heliyon, vol. 8, no. 12, p. e11912, Dec. 2022, doi: 10.1016/J.HELIYON.2022.E11912.

[7] D. K. V. Sagiraju, Y. P. Obulesu, and S. B. Choppavarapu, "Dynamic performance improvement of standalone battery integrated PMSG wind energy system using proportional resonant controller," Engineering Science and Technology, an International Journal, vol. 20, no. 4, pp. 1353–1365, Aug. 2017, doi: 10.1016/J.JESTCH.2017.03.010.

[8] A. Azizi, H. Nourisola, and S. Shoja-Majidabad, "Fault tolerant control of wind turbines with an adaptive output feedback sliding mode controller," Renew Energy, vol. 135, pp. 55–65, May 2019, doi: 10.1016/J.RENENE.2018.11.106.

[9] P. K. Gayen, "Magnetizing current based improved rotor position and speed estimation of doubly-fed induction generator using model reference adaptive scheme," Measurement, vol. 173, p. 108602, Mar. 2021, doi: 10.1016/J.MEASUREMENT.2020.108602.

[10] G. Rigatos and P. Siano, "DFIG control using Differential Flatness theory and Extended Kalman Filtering," IFAC Proceedings Volumes, vol. 45, no. 6, pp. 1763–1770, May 2012, doi: 10.3182/20120523-3-RO-2023.00015.

[11] M. A. S. Ali, K. K. Mehmood, S. Baloch, and C. H. Kim, "Modified rotor-side converter control design for improving the LVRT capability of a DFIG-based WECS," Electric Power Systems Research, vol. 186, p. 106403, Sep. 2020, doi: 10.1016/J.EPSR.2020.106403.

[12] H. T. Jadhav and R. Roy, "A comprehensive review on the grid integration of doubly fed induction generator," International Journal of Electrical Power & Energy Systems, vol. 49, no. 1, pp. 8–18, Jul. 2013, doi: 10.1016/J.IJEPES.2012.11.020.

[13] K. Reddy and A. K. Saha, "A review of swarm-based metaheuristic optimization techniques and their application to doubly fed induction generator," Heliyon, vol. 8, no. 10, p. e10956, Oct. 2022, doi: 10.1016/J.HELIYON.2022.E10956.

[14] A. Kasbi and A. Rahali, "Performance improvement of modern variable-velocity wind turbines technology based on the doubly-fed induction generator (DFIG)," Mater Today Proc, vol. 45, pp. 5426–5432, 2021, doi: https://doi.org/10.1016/j.matpr.2021.02.114.

[15] A. B. Tadesse, E. A. Ayele, and A. O. Olonje, "Design and Analysis of Rate Predictive Fractional-Order Sliding Mode Controller (RP-FOSMC) for MPPT and Power Regulation of DFIG-based Wind Energy Conversion System (WECS)," Energy Reports, vol. 8, pp. 11751–11768, 2022, doi: https://doi.org/10.1016/j.egyr.2022.09.026.

[16] S. Rajendran, M. Diaz, R. Cárdenas, E. Espina, E. Contreras, and J. Rodriguez, "A Review of Generators and Power Converters for Multi-MW Wind Energy Conversion Systems," Processes, vol. 10, no. 11. 2022. doi: 10.3390/pr10112302.

[17] K. E. Okedu, M. Al Tobi, and S. Al Araimi, "Comparative study of the effects of machine parameters on DFIG and PMSG variable speed wind turbines during grid fault," Front Energy Res, vol. 9, 2021.

[18] M. S. Haider Khan and S. Kumar Mallik, "Mechanical sensorless control of a rotor-tied DFIG wind energy conversion system using a high gain observer," Journal of King Saud University - Engineering Sciences, May 2022, doi: 10.1016/J.JKSUES.2022.05.005.

[19] R. Patel, F. Hafiz, A. Swain, and A. Ukil, "Nonlinear rotor side converter control of DFIG based wind energy system," Electric Power Systems Research, vol. 198, p. 107358, Sep. 2021, doi: 10.1016/J.EPSR.2021.107358.

[20] M. A. S. Ali, K. K. Mehmood, S. Baloch, and C. H. Kim, "Modified rotor-side converter control design for improving the LVRT capability of a DFIG-based WECS," Electric Power Systems Research, vol. 186, p. 106403, Sep. 2020, doi: 10.1016/J.EPSR.2020.106403.

[21] D. S. L. Simonetti, A. E. A. Amorim, and F. D. C. Oliveira, "Doubly Fed Induction Generator in Wind Energy Conversion Systems," in Advances in Renewable Energies and Power Technologies, Elsevier, 2018, pp. 461–490. doi: 10.1016/B978-0-12-812959-3.00015-0.

[22] H. Abu-Rub, M. Malinowski, and K. Al-Haddad, Power Electronics for Renewable Energy Systems, Transportation and Industrial Applications, vol. 9781118634035. 2014. doi: 10.1002/9781118755525.

[23] A. Mohammad Nezhad, B. Tousi, and F. Sabahi, "Power Control of a Grid-Connected Doubly Fed Induction Generator Using H ∞ Control and Kalman Filter," International Transactions on Electrical Energy Systems, vol. 2022, p. 3771752, 2022, doi: 10.1155/2022/3771752.

[24] L. A. G. Gomez, L. F. N. Lourenço, M. B. C. Salles, A. P. Grilo, and A. J. S. Filho, "Chapter 19 - Frequency support by grid connected DFIG-based wind farms," in Advances in Nonlinear Dynamics and Chaos (ANDC), A. T. Azar and N. A. B. T.-D. Kamal Analysis, and Applications of Renewable Energy Systems, Eds., Academic Press, 2021, pp. 481–496. doi: https://doi.org/10.1016/B978-0-12-824555-2.00025-3.

[25] S. Li, Y. Li, X. Chen, W. Jiang, X. Li, and T. Li, "Control strategies of grid-connection and operation based on active disturbance rejection control for virtual synchronous generator," International Journal of Electrical Power & Energy Systems, vol. 123, p. 106144, 2020, doi: https://doi.org/10.1016/j.ijepes.2020.106144.

[26] Y. Ling and X. Cai, "Rotor current dynamics of doubly fed induction generators during grid voltage dip and rise," International Journal of Electrical Power & Energy Systems, vol. 44, no. 1, pp. 17–24, 2013, doi: https://doi.org/10.1016/j.ijepes.2012.07.032.

[27] P. K. Gayen, D. Chatterjee, and S. K. Goswami, "Stator side active and reactive power control with improved rotor position and speed estimator of a grid connected DFIG (doubly-fed induction generator)," Energy, vol. 89, pp. 461–472, 2015, doi: https://doi.org/10.1016/j.energy.2015.05.111.

[28] Z. Zabar, "Electric Machines, Drives," R. A. B. T.-E. of P. S. and T. (Third E. Meyers, Ed., New York: Academic Press, 2003, pp. 69–95. doi: https://doi.org/10.1016/B0-12-227410-5/00917-0.